

Alex Pokryvailo and Cliff Scapellati

*Spellman High Voltage Electronics Corporation
475 Wireless Boulevard
Hauppauge, NY 11788*

Behavior of HV Cable of Power Supply at Short Circuit and Related Phenomena

Copyright © 2013 IEEE. Reprinted from IEEE Transactions on Dielectrics and Electrical Insulation Vol. 20, No. 1; February 2013

This material is posted here with permission of the IEEE. Such permission of the IEEE does not in any way imply IEEE endorsement of any of Spellman High Voltage Electronics Corporation's products or services. Internal or personal use of this material is permitted. However, permission to reprint/republish this material for advertising or promotional purposes or for creating new collective works for resale or redistribution must be obtained from the IEEE by writing to pubs-permissions@ieee.org.

By choosing to view this document, you agree to all provisions of the copyright laws protecting it.

Behavior of HV Cable of Power Supply at Short Circuit and Related Phenomena

Alex Pokryvailo and **Cliff Scapellati**

Spellman High Voltage Electronics Corporation
475 Wireless Blvd.
Hauppauge NY 11788, USA

ABSTRACT

Discharges in many HV loads are unavoidable at voltages close to their operational limits. Such loads may be vacuum gaps, e.g., X-ray tubes. The discharge characteristics depend not only on the state of the load, but, in the case of a vacuum gap, on external circuitry. In cabled connections, the cable length is critical. Long cables may decrease the breakdown voltage, which is mostly overlooked in literature. Selected experimental data and means of improving performance are reviewed. Regarding methods of cable connections, we consider two cases. In the first, regular connection, the cable shield is connected to ground on both sides. Then the processes in the cable can be described by conventional transmission line equations. Pattern of traveling waves developing at short-circuit conditions and overvoltages (OV) at the power supply side are shown as a function of the cable parameters. In the second case, the shield at the power supply side is grounded, and at the load side it is floating (unterminated shield connection). It is shown that conventional two-wire transmission line model is no longer applicable. PSpice equivalent circuits with lumped parameters are developed and analyzed. It is shown that the cable insulation is overstressed at the load side in unterminated shield connections, and at the power supply side in regular connections. Experimental results obtained on low-voltage models are presented.

Index Terms - High-voltage cable, insulation, short-circuit, overvoltages, X-ray tube.

1 INTRODUCTION

1.1 GENERAL

DISCHARGES in HV loads at voltages close to their operational limits are virtually unavoidable. Such loads may include devices operating in vacuum, and in particular, X-ray tubes. The discharge characteristics depend not only on the load, but, to a large extent, on the external circuitry, namely, the capacitance directly connected to the load, and limiting impedance, if any. The influence of external circuit is most strongly expressed in the case of vacuum loads and is much less felt in atmospheric pressure gas loads.

Often the load is connected to the high voltage power supply (HVPS) via a long HV cable. The cable can have its shield a) grounded on both sides or b) only at the HVPS side. We will term the latter as “unterminated shield connection”. For the clarity sake, we note that only coaxial cables are considered in this paper. In this category also

fall the cables with several central conductors that can be used for filament and grid supplies. In the case a) the processes in the cable can be described by conventional transmission line equations (see, e.g., [1], [2]). It will be shown that in unterminated shield connections, these equations are inapplicable “as is”. We are unaware of analyses of such connections in literature.

1.2 VACUUM LOAD

As noted above, we single out vacuum gaps because their discharge characteristics are most sensitive to the feeding scheme. The authors are well familiar with X-ray tubes and their HVPS; this why we focus further on these devices.

Although the theory of discharge in vacuum is far from being complete [3]-[8], from the angle of electromagnetic interference (EMI) we will distinguish between a) microdischarges and b) spark discharges. (Here, we follow mostly the terminology of [3], [8].) The first are characterized by minor voltage drops, whereas spark fully discharges the capacitances connected to the load. We will term the sum of these capacitances as “output capacitance”, C_{out} . Spark may transit to arc if HVPS does

not limit the current below a certain level or does not shut down.

Microdischarges may be weak (milliamperes) and as such do not create serious disturbance. However, more intense microdischarges are also common [3] (see also [8] p. 24). The load voltage does not collapse fully, but the spurious discharge currents are much stronger, exceeding ampere levels, and may lead to malfunctioning of sensitive electronics [9]. Microdischarges in X-ray tubes are often related to presence of residual gas.

Sparks are associated with short μs current pulses that may be many kA in amplitude. The time of the current rise depends on the velocity of the plasma front bridging the gap. There is a consensus now based on a large body of experimental work that this velocity is typically 2 cm/ μs for cm-long gaps. Thus, the “closure” time of a vacuum gap can be estimated from the above considerations with high confidence; the current risetime is, obviously, shorter, depending also on capacitance C_{out} directly connected to the electrodes. The current amplitude I_m increases with C_{out} and, by one of the popular theories, is approximately proportional to C_{out}^2 starting from a certain value of C_{out} : $I_m \sim C_{out}^2$ [10].

We note that in liquid and solid dielectrics breakdown develops much faster than in vacuum. This is also true for gases at relatively high pressure. For instance, in air at atmospheric pressure and higher, moderate-length gaps are bridged much faster because of high speed of streamer propagation (of the order of 10^7 - 10^8 cm/s at atmospheric pressure, depending on gap and voltage parameters; see, for example, [11], [12] and their bibliography) and faster spark development.

Yet another important feature of spark breakdown in vacuum is the decrease of the breakdown voltage, V_{br} , with the increase of C_{out} . In X-ray apparatus, V_{br} drops dramatically when a long HV cable is used. We observed, for instance, that with a 15-m cable with rubber insulation V_{br} dropped from 70 kV to below 55 kV for a tube rated at 70 kV. With other tubes, V_{br} was 25-35 kV and 45-50 kV with 9-m and 3-m cable, respectively [9].

A convincing proof of the influence of the external circuitry on the breakdown voltage of a vacuum gap was given in [3] (see also [13]). It was found that even a small resistance separating C_{out} from the gap increases V_{br} by tens of percent. Likewise, reduction of stored energy also acted favorably on the dielectric withstand of *conditioned* gaps. Our experimental work is in line with these findings (see Section 4).

1.3 INFLUENCE OF HV CABLE LENGTH ON ELECTROMAGNETIC PROCESSES

When accounting for the HV cable influence on electromagnetic processes, a simplest approximation would be representing the cable by a lump capacitance. This simplification works quite well for almost all scenarios except short transient phenomena, the reason for the latter being that the cable electrical length may be commensurable with the time of the gap flashover. In this

case, it is more correct to represent the cable as a transmission line with characteristic impedance Z and speed of propagation v (losses can be neglected unless the cable is very long). Speed of propagation is $v = c/\sqrt{\epsilon}$, where ϵ is relative permittivity of the cable insulation, on condition that the cable does not contain ferromagnetic materials; c is speed of light. In this section, we adopt the values $Z=59 \Omega$, and $\epsilon=3.15$. The first is taken from the specifications of a 2042 Dielectric Sciences cable [14], and the second is a value calculated from the cable capacitance and geometry, again for the same cable. Thus, the time it takes for the wave to travel 1m in a 2042 cable is $\tau=5.3$ ns.

With a short cable, all transients may decay before the gap has been bridged by plasma, and the discharge may not transit to a spark. With longer cables, there is more time for the plasma propagation at conditions of sustainment by the cable energy. Let us analyze an example. For a 2-cm gap, typical for some X-ray tubes rated at 150 kV, the time that takes to plasma to fully bridge the gap is $\sim 1 \mu\text{s}$, and it is considerably smaller for gas gaps at atmospheric and higher pressure. The current risetime is considerably shorter [3], [6]-[8]. A 3-m cable is able to sustain the discharge for only about $3\tau \approx 16$ ns, whereas a 15-m long cable makes it 79 ns. We note that a 3-m cable can be “short” for a vacuum load, but be quite “long” for a high-pressure gas-discharge load. These arguments, even though oversimplified, indicate to a critical importance of the cable length.

We note that the cable limits the discharge current to a value of $I_m = V/Z$, where V is the charge voltage.

The mere presence of long HV cables has tremendous influence on dielectric behavior of HV loads, especially, vacuum gaps, and OV in HVPS resulting from load breakdown. The nature and magnitude of OV depend on the method of the cable connection. These factors, mostly overlooked in literature, are addressed in the following sections (see also [15]).

2 BASIC ANALYSIS OF TRANSIENT PHENOMENA WITH SHIELD GROUNDED ON BOTH ENDS (REGULAR CONNECTION)

In many HV systems the cable shield is grounded on both ends. Then, if the load is short-circuited, the cable discharges in such a way that both the voltage and current are reflected from both ends with polarity reversal. The process repeats itself until all the energy dissipates, mainly as heat. This case has an analytical solution that can be found elsewhere [16], [17]. We use PSpice simulations. Multiple reflections are illustrated by the waveforms of Figure 1. Here we assume that the charging power supply V1 is isolated from the cable, which is typical of HVPS having arc-limiting means. Notably, the voltage at the cable start contains a high-frequency component detrimental for insulation.

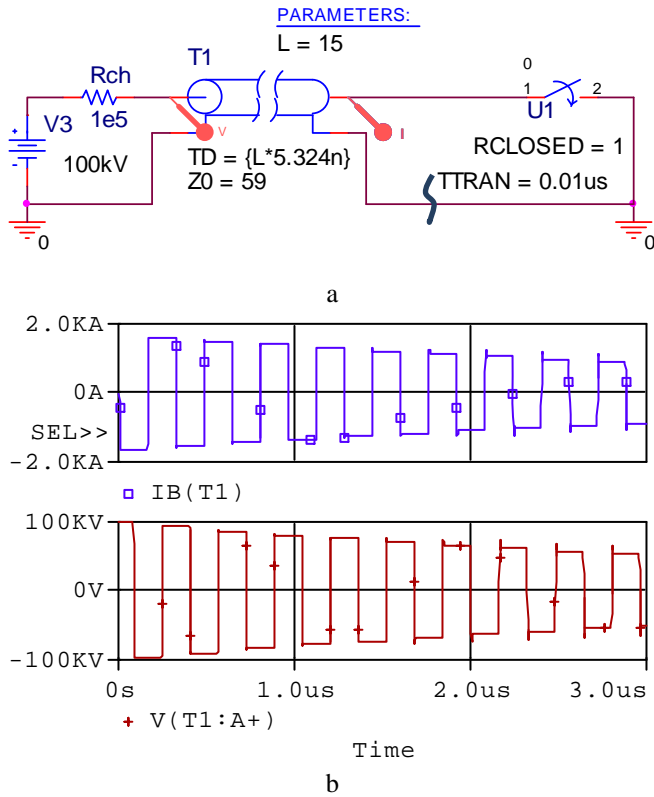


Figure 1. a - PSpice model of 15-m 2042 cable discharge on short circuit. Switch closing/transition time, TTRAN, is a PSpice parameter; it is much shorter than cable electrical length. b – timing diagrams. Current amplitude is V/Z.

If the line is shorter, and/or the transition time is larger, the reflections are less intense. They disappear below some critical length, in this case below 3m. Figure 2 shows the dependence of the peak reversal voltage and peak discharge current on the cable length (referenced to charge voltage of 100 kV). It is seen that both the peak reversal voltage and peak discharge current tend to their theoretical limits at larger lengths.

3 TRANSIENT PHENOMENA AT UNTERMINATED SHIELD CONNECTION

3.1 THEORETICAL

The cable shield is not grounded at the load side in many applications, e.g., electrostatic precipitation and ion implantation, and in HV testing and general laboratory practice. It appears that notwithstanding the practical importance of this case, no analyses are available in open literature.

A basic assumption in deriving telegraphic equations for a two-conductor transmission line is that both conductors carry only differential currents that are equal to each other in every point [1], [2], [16]. Incidentally, the PSpice TL models presuppose that this is the case, hence trying to insert an impedance between the shield and ground on one end yields absurd results. However, unterminated shield connection presents exactly such a situation! If the shield is lifted off ground as shown by the curved line in Figure 1, shield current

at this end is zero, but its counterpart in the central conductor is not. Actually, in unterminated shield connection we deal with a three-conductor transmission line, the third conductor being ground. On the next level of complexity, we note that such a line may not support TEM modes if the cable is far from ground, which means that the cross-sectional distances are commensurable with wavelength. In this case, the shield may act as an antenna. However, neglecting displacement currents flowing from the shield to ground and between adjacent parts of the shield itself (in the instance of a coiled cable), we can stay within a convenient simplicity of a two-wire line approximation. It will be seen that such a simplification still allows analyzing salient phenomena of the load breakdown in unterminated shield connection.

We will use lumped circuit modeling, one of the reasons being that it allows PSpice modeling. First, we take a look at traditional equivalent circuit used for deriving telegraph equations Figure 3. Such circuits (PFNs) are also used for generation of rectangular pulses. Note that the return conductor is just a wire; all impedances are lumped into the forward conductor, and thus, the currents in both are equal. We cannot use such a model to have zero current through the isolated shield at distal end at short circuit. Rather, we halve the inductance between the forward and return conductors, so that the total cell inductance remains the same. Figure 4a shows such a model for a 10-m RG-58/U cable (neglecting losses), whereas Figure 4b is the same in conventional representation.

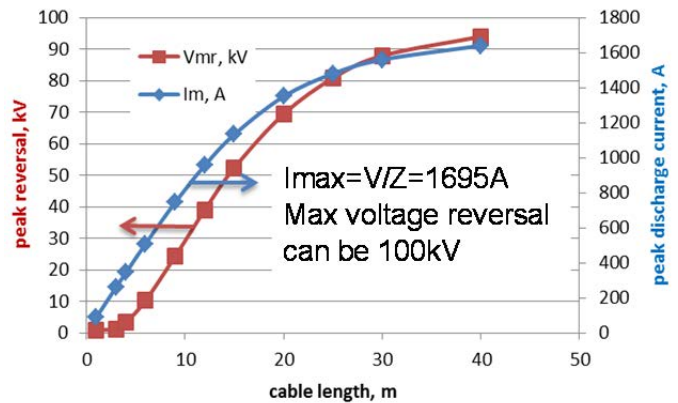


Figure 2. Dependence of peak reversal voltage and peak discharge current (V(T1:A+) and IB(T1), respectively, per notation of Figure 1) on cable length (referenced to charge voltage of 100 kV). In these simulations, TTRAN=1 μs (actual transition from 90% to 10% is 200ns).

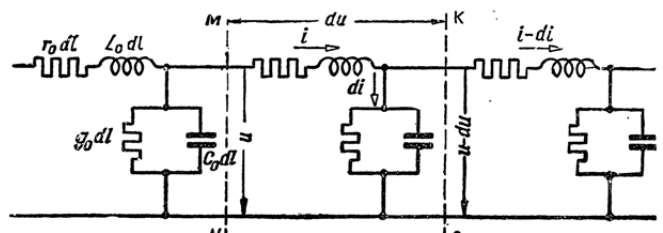


Figure 3. Lumped representation of two-wire TL (copied from [16]). L_0 , C_0 , r_0 and G_0 are TL inductance, capacitance, resistance and conductance, respectively, per unit length.

Figure 5 shows simulation results for the circuits Figure 4a, b for $R_6=10^{-9}\Omega$, i.e., shield grounded at distal end. Circuit Figure 4b generates usual quasi-rectangular waveforms (compare to their experimental counterparts below) as any PFN would. However, circuit Figure 4a, differing only in that the cell inductance is just split in two, defying common sense, generates triangular rather than rectangular waveforms.

Figure 6 is a simulation of circuit Figure 4a for $R_6=10^9\Omega$ (unterminated shield connection). It is seen that the shield voltage at distal end jumps to the supply voltage upon the switch closure and then starts oscillating. Thus, in an unterminated shield connection, the insulation on both sides of the cable is subjected to full voltage reversals. This puts large stress on the cable terminations [18].

3.2 EXPERIMENTAL

A low-voltage test rig schematic diagram is shown in Figure 7. Two sections of ~5.5-m-long RG-58 cables (total length~11m, electrical length ~58 ns) joined with a BNC Tee were charged up to 60 V through a high-value limiting resistor. The cable was coiled and put on an aluminum plate that was connected to system ground. The TL was discharged in a repetitive mode to ground using a fast MOSFET IRFD110 (actual switching time with hard gating - no gate resistor - was <5 ns—see Figure 8). TL voltages were monitored by a DPO7054 scope with 400 MHz P6139A probes in three points: at TL start $V(0)$, at half-length $V(d/2)$, and distal end $V(d)$.

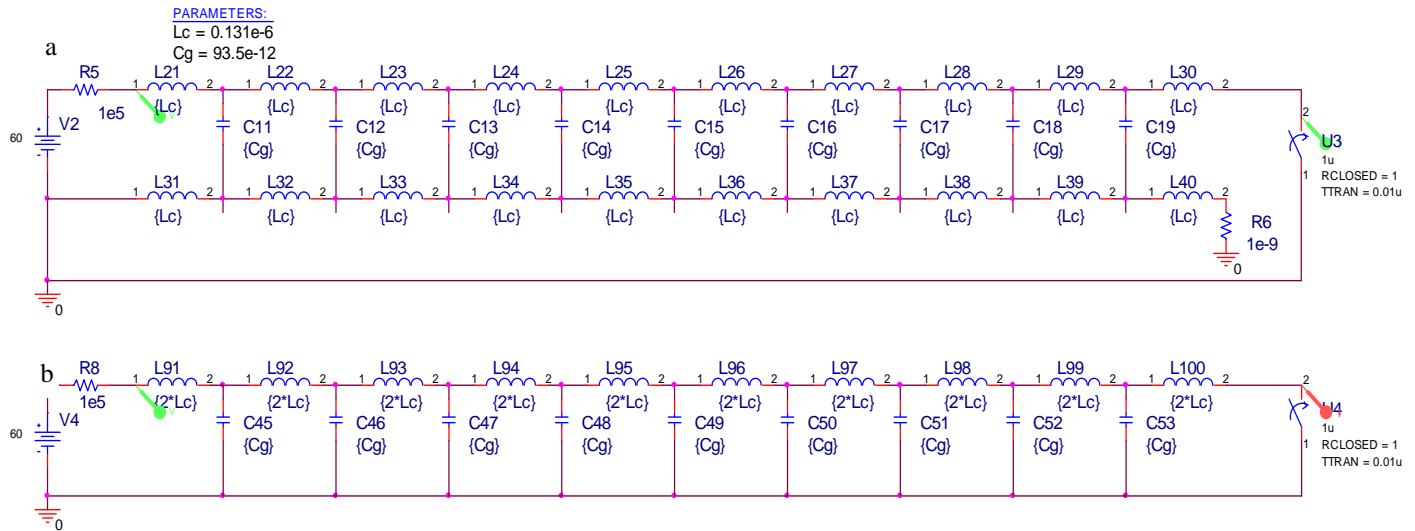


Figure 4. Lumped PSpice model of a 10-m RG-58/U cable. a – shield isolated at distal end. Cell inductance is split in two; b – conventional model lossless transmission line model. RG-58/U parameters taken from Belden catalog [19]: $L=262\mu\text{H/m}$, $C=93.5\text{pF/m}$.

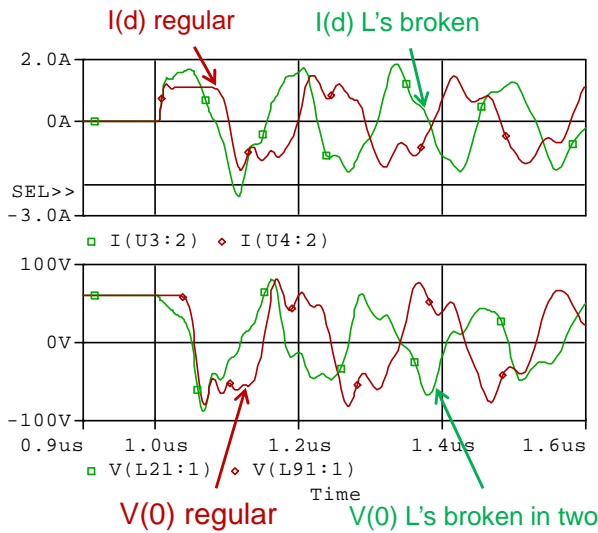


Figure 5. Simulation of circuit Figure 4. $R_6=10^{-9}\Omega$ (shield at distal end grounded).

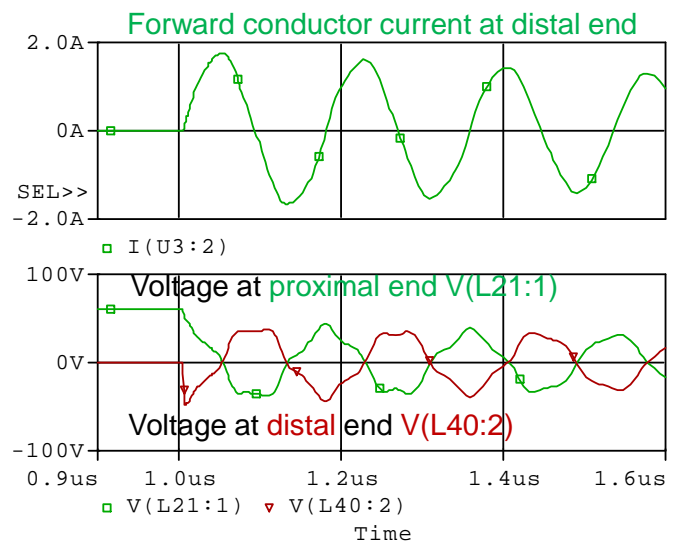


Figure 6. Simulation of circuit Figure 4a. $R_6=10^9\Omega$ (shield at distal end isolated).

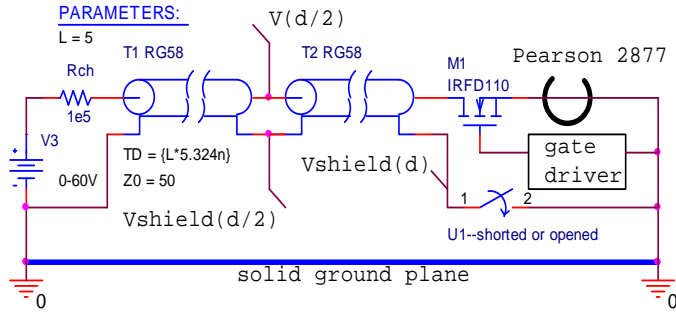


Figure 7. Experimentation scheme.

The shield potential at these points is denoted as $V_{shield}(0)$, $V_{shield}(d/2)$ and $V_{shield}(d)$, respectively. In addition, the current at the distal and/or proximal end was monitored with Pearson 2877 and 2878 current transformers (risetime 2 ns and 4 ns, respectively). Note that coiling the cable and placing it on a grounded plane introduces considerable capacitance of the cable shield to both ground and between the adjacent parts of the shield itself.

A reference experiment was shorting the line with shield connected to ground at distal end. Figure 9 exhibits the waveforms, with expected quasi-rectangular pulses and almost full reversal of voltage and current at proximal and distal ends, respectively.

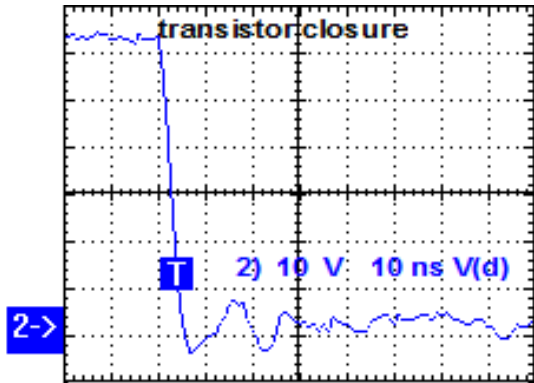


Figure 8. Transistor closure. Waveform annotation here and further gives scales' information (vertical – 10 V/div, horizontal – 10 ns/div) and legend.

With shield isolated from ground at the distal end, the picture is entirely different. Since the shield electric charge cannot disappear instantly, full line voltage is generated between shield and ground at distal end. Traveling waves with full voltage reversal decay slowly at this end. Thus, the cable insulation in unterminated shield connections is subjected to a detrimental stress if load sparks. As shown in [18], the insulation at the shield termination is highly vulnerable, and certainly suffers from high-frequency voltage components. The shield can also spark to ground inducing intense EMI aggravated by the fact that the current discharge loop tends to be large. The radiated field may have detrimental results at the system level. Detailed analysis of such effects is beyond the scope of this paper.

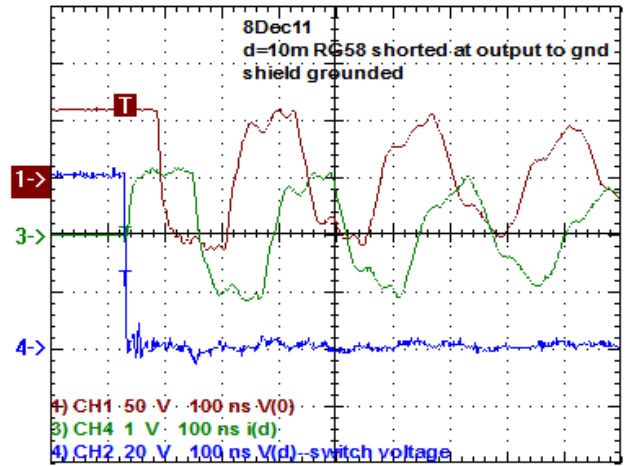


Figure 9. Short to ground, shield shorted at both proximal and distal ends. Trace 1 (Ch1) – voltage at proximal end; Trace 3 (Ch4) – current at distal end 1 A/div; Trace 4 (Ch2) – voltage at distal end (switch voltage). Horizontal – 100 ns/div.

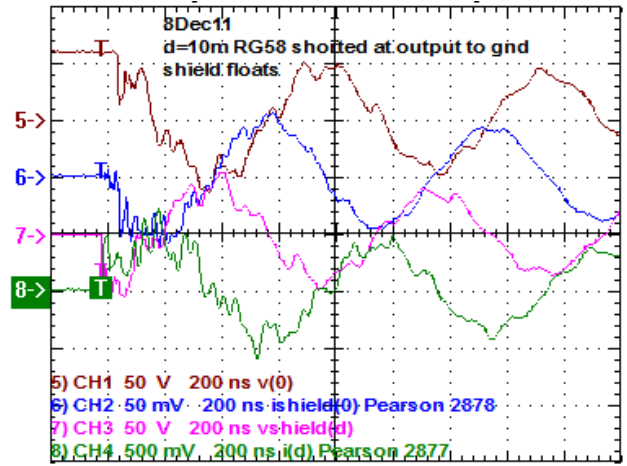


Figure 10. Short to ground, shield floats at distal end. Trace 5 (Ch1) – voltage at proximal end; Trace 6 (Ch2) – current at distal end 0.5 A/div; Trace 7 (Ch3) – shield voltage at distal end; Trace 8 (Ch4) – current at distal end 0.5 A/div; Horizontal – 200 ns/div.

4 MEANS OF INCREASING THE BREAKDOWN VOLTAGE

Usually, HVPS have arc limiters installed at the output *before* the HV cable. They limit the current generated by discharge of the energy stored in the output stages of the HVPS to a level safe both to the load and HVPS itself. In the simplest case, arc limiter is an HV surge resistor. More sophisticated limiters comprised of inductors, resistors, etc., are also used, especially, in high-current HVPS. However, conventional limiters do not prevent energy flow from the cable, which decreases V_{br} , as noted in previous sections. An obvious solution to this problem would be installation of a current-limiting device between the cable and the load. Technical difficulties here are of two kinds. First, space is extremely limited. Second, in X-Ray apparatus, the filament is usually fed by high-frequency current, and the limiter must pass the filament current without generating prohibitively high voltage drop and power losses.

A means of increasing the breakdown voltage of an X-ray tube fed by an HVPS via a long cable is shown in Figure 11. The limiter electrical and mechanical design, implementation and testing were described in [9], [20]; see also [21] for yet another circuit design. In one of the X-Ray generators, a 35-mm-diameter, 40-mm-long two-winding choke had an inductance of $L_{ch}=200\mu\text{H}$ (measured on one winding). It presented a very low impedance to the filament current but high impedance to discharge current. Assuming that the characteristic frequency of the latter is $f=1\text{ MHz}$, which corresponds to risetime of fractions of a microsecond, we calculate $Z=2\pi fL_{ch}=1.256\text{ k}\Omega$. (Similar and even lower value resistances were very effective in suppressing breakdown in vacuum [3].) The choke was installed in the tube shield between the cable bushing and the tube. It virtually abolished the tube *microdischarges* that otherwise severely destabilized operation. Indirectly, the effectiveness of current limitation was judged by measuring electromagnetic pickup with a $\sim 500\text{ cm}^2$ loop antenna placed in the vicinity of the HV cable. Without the choke, typical pickup signal was 10 V, and with the choke the amplitude dropped by two orders of magnitude, and the frequency of the events was also orders of magnitude lower.

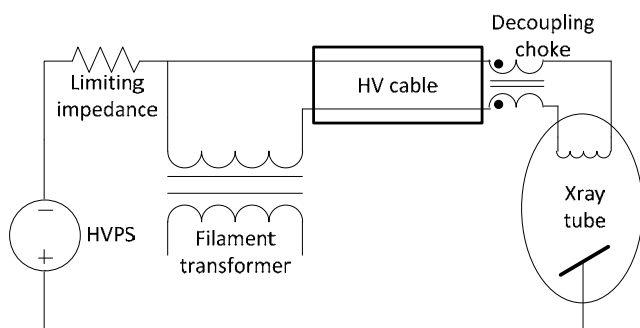


Figure 11. Common-mode choke as an arc-limiter in X-Ray HVPS.

5 CONCLUSIONS

1. The designer should be aware of problems caused by long HV cables. These problems are low breakdown voltage, high insulation stresses and high EMI. Whereas the latter is more evident (more energy is stored, the higher are the discharge currents), the first two factors are commonly disregarded.
2. In regular connection making use of long HV cables, insulation is overstressed by rapid voltage reversals at the HVPS side.
3. In unterminated shield connection, phenomena at short-circuit are not readily described by telegraph equations; cable insulation is overstressed by rapid voltage reversals at the load side. In this case, if long cable is used, its termination should be designed more carefully compared to regular connection.
4. The load breakdown voltage can be considerably increased by inserting a low-value impedance between the cable and the load. For high-current loads, small-value inductors (tens - hundreds μH) are quite effective.

REFERENCES

- [1] G. Miano and A. Maffucci, *Transmission Lines and Lumped Circuits*, Academic Press, NY, 2001.
- [2] C. R. Paul, *Analysis of Multiconductor Transmission Lines*, Wiley, NY, USA, 2008.
- [3] I.N. Slivkov, *Electrical Breakdown of Vacuum*, Energoatomizdat, Moscow, Russia, 1972 (In Russian).
- [4] J.M. Lafferty, Ed., *Vacuum Arcs*, Wiley, 1980.
- [5] R.L. Boxman, D. M. Sanders and P. J. Martin, Editors, *Handbook of Vacuum Arc Science and Technology*, Noyes Publications, NJ, USA, 1995.
- [6] G.A. Mesyats, "Ectons". In three parts, Nauka, Ekaterinburg, 1993 (in Russian).
- [7] G.A. Mesyats and D.I. Proskurovski, *Pulsed Electrical Discharge in Vacuum*, Springer-Verlag, 1989.
- [8] R. Latham, *High Voltage Vacuum Insulation*, Academic Press, San Diego, USA, 1995.
- [9] A. Pokryvailo, K.K. Vlasov, Yu. A. Magdin and A.N. Starchikov, "On the Electromagnetic Compatibility of High Voltage Power Supplies for X-Ray Analytical Apparatus Operating under Conditions of High Voltage Discharges", *Instrumentation and Methods of X-Ray Analysis*, Vol. 40, pp. 151-158, 1990.
- [10] P.T.G. Flynn, "The Discharge Mechanism in a Cold Cathode Pulsed X-Ray Tube", *Proc. Phys. Soc. B (UK)*, Vol. 69, pp. 748-762, 1956.
- [11] E.M. Bazelyan and Yu.P. Raizer, *Spark Discharge*, CRC Press, NY, USA, 294 pp, 1998.
- [12] Yu. Raizer, *Gas Discharge Physics*, Springer, Berlin, Germany, 1991.
- [13] R. Hackam, "Effects of voltage polarity, electric current, external resistance, number of sparkings, supply frequency, and addition of hydrogen and air on electrical breakdown in vacuum", *J. Appl. Phys.*, Vol. 46, pp. 3789-3799, 1975.
- [14] <http://dielectricsciences.thomasnet.com/Asset/2042.pdf>
- [15] A. Pokryvailo, and C. Scapellati, "Behavior of HV Cable at Short Circuit and Related Phenomena", *IEEE Int'l. Power Modulator and High Voltage Conf. (IPMHVC)*, San Diego, USA, Paper 307, 2012.
- [16] K. A. Krug, *Foundations of Electrotechnics*, 6th ed., Vols. 1 and 2, Gosenergoizdat, Moscow, Russia, 1946.
- [17] G. A. Mesyats "Pulsed Power and Electronics", Moscow, Nauka, 2004 (in Russian). Translation to English: *Pulsed Power*, Kluwer, NY, 2005.
- [18] A. Pokryvailo, C. Carp and C. Scapellati, "Comparative Testing of Simple Terminations of High Voltage Cables", *IEEE Electr. Insul. Mag.*, Vol. 26, No. 1, pp. 7-17, 2010.
- [19] RG 58/U cable <https://edskv2.belden.com/Products/index.cfm?event=showproductdetail&partid=1979>
- [20] A. Pokryvailo, and V. Resnik, "X-Ray Generator", Soviet Patent A.C.1628235, 1990.
- [21] A. Pokryvailo, and A. Starchikov, "X-Ray Generator", Soviet Patent A.C.1220141, 1985.



Alex Pokryvailo (M'05-SM'07) was born in Vyborg, Russia. He received the M.Sc. and Ph.D. degrees in electrical engineering from the Leningrad Polytechnic Institute in 1975 and 1987, respectively. Formerly with Soreq NRC, Israel, now he is with Spellman High Voltage Electronics Corp., serving as Director of Research. His current and recent experience relates to design of HV high-power switch-mode power supplies, Pulsed Power, with emphasis on high-current

opening and closing switches and magnetic design, fast diagnostics, and corona discharges. Previously, he studied switching arcs, designed SF6-insulated switchgear, made research in the area of interaction of flames with electromagnetic fields, etc. He published over 120 papers, two textbooks (in Hebrew), and more than 20 patents pertaining to HV technology.

Cliff Scapellati (M'92), photograph and biography not available at the time of publication.